A Prograde Jet Driven by Rossby Waves

RORY O. R. Y. THOMPSON[1]

Oceanography Department, Florida State University, Tallahassee, FL 32306

(Manuscript received 4 December 1979, in final form 8 February 1980)

ABSTRACT

Waves are forced by moving sources and sinks of mass on a beta-plane with Ekman friction. If the motion is retrograde and not too fast, these are Rossby waves with a nonzero Reynolds stress $\overline{u'v'}$. This stress forces a meridional mass flux which builds up a pressure gradient to allow a compensating mass flux in the Ekman layer. In a rotating system, this meridional pressure gradient requires a zonal flow

$$\tilde{u}(y) = -\frac{\partial}{\partial y}(\overline{u'v'})/E^{1/2}\Omega,$$

which is also the momentum accumulated by the Reynolds stress in one spindown time. An example shows how excitation of Rossby waves brings momentum into the source of energy, causing a prograde jet there, with retrograde currents on each side. A laboratory experiment confirms the theory, which is proposed as an explanation of the observed "negative viscosity" of the jet stream in the atmosphere and the Gulf Stream in the ocean.

1. Introduction

It has been known since Starr and White (1951) that the strongest currents in the atmosphere are driven by Reynolds stresses of geostrophic waves. This means that momentum flows upgradient *into* the regions of maximum relative momentum. This "negative viscosity" has been thoroughly documented and referenced by Starr (1968); also, see Holopainen (1978) and Thompson (1978). A physical explanation of this odd behavior was given by Thompson (1971), who argued that the meridional phase and group velocities of Rossby waves are of opposite sign, so an outward propagation of energy from a zone requires an inward propagation of momentum. In the atmosphere and ocean the source of energy for the waves is baroclinic instability, which involves stratification and horizontal and vertical shears. To simplify the problem to the essentials, we will consider a homogeneous, barotropic fluid on a beta-plane, with the baroclinic instability represented by direct driving of the waves. The experiment was done in a rotating cylinder, so we also will have to consider the effects of a cylinder.

There have been numerous theoretical contributions to an explanation of "negative viscosity." Taylor (1915) related the momentum flux gradient and the vorticity flux by eddies. Kuo (1951a,b, 1953) applied Taylor's theory to get the acceleration for the mean flow on an inviscid, barotropic beta-plane, i.e.,

$$\frac{\partial \bar{u}}{\partial t} = -\frac{\beta}{2}\frac{d}{dt}(\overline{\eta^2}), \tag{1.1}$$

where u is the zonal flow, the bar is a zonal average, and η is the meridional displacement of a particle from its original latitude. He concluded that westerlies will spring up within a disturbed zone (i.e., cyclone belt) and easterlies outside. Eliassen and Palm (1960) considered the relationship between momentum flux and energy flux for stationary waves, and showed that there can be no interaction between steady waves and a mean flow without friction or critical layers. Green (1970) gave reasonable arguments to show that meridional mixing of entropy and potential vorticity can force an upgradient flux of momentum. Held (1975) showed that, in an inviscid but baroclinic system, if there is an increase of mean-square eddy vorticity in a zonal band, there is a convergence of momentum toward that zone. A clear account by Rhines (1977, 1979) is apparently the first to explicitly include friction. Rhines showed that the mean flow is everywhere retrograde outside of the zone of eddy forcing, but was not able to prove there would be a prograde jet in the forced region. McEwan *et al.* (1981) found that for forcing of the sort considered by Eliassen and Palm (1960), there is in fact no prograde jet. They further compute the theoretical jets for source-sink forcing

[1] Current affiliation: CSIRO Division of Oceanography, Box 21, Cronulla, Australia 2230.

0022-4928/80/061216-11$06.75

over uniform Ekman friction. De Verdiere (1979) proposed that a sideband instability will cause zonal flows, but does not specify the resultant sense nor magnitude.

Except for the last, the above theories have been based on vorticity transport and are at least partially Lagrangian. The present paper uses an Eulerian derivation, and concentrates on the role of the Ekman layer in setting up a steady mean flow. While the results are similar to those of McEwan *et al.* (1980), the derivation presents quite a different view of the dynamics.

There have been many numerical experiments which have exhibited "negative viscosity," but only three seem obviously relevant to the present study. In the early sixties, E. N. Lorenz (unpublished personal communication) ran models of inviscid barotropic flow on a sphere and found that zones with initially high eddy energy acquired mean prograde zonal flow. Mak (1969) ran a dissipative two-layer equatorial beta-plane, forced stochastically at the edges, and found a strong equatorial energy flux, a strong poleward momentum flux, and mean easterlies everywhere between the edges (i.e., retrograde zonal flow). Williams (1978) ran models of dissipative barotropic flow on a sphere with stochastic forcing at midlatitudes, and got very pretty results, with westerly (prograde) jets in the forced zones and broad easterlies (retrograde) in the unforced zones.

There seem to have been three laboratory experiments designed to look for mean zonal flow generation by directly forced geostrophic eddies, all in "polar beta-plane", that is, a rotating cylinder with a flat bottom and free, hence paraboloidal, surface. Whitehead (1975) oscillated a disk vertically at mid-depth and mid-radius, and got some nice Rossby waves and a prograde mean zonal flow at approximately the radii of the forcing and retrograde elsewhere. Whitehead also replaced the disk by a source of air bubbles, and observed the same sort of zonal flows but no waves. Apparently, in this case, the buoyance of the bubbles drove mean meridional Hadley cells, as evidenced by the potassium permanganate patterns on the bottom, with consequent zonal flows being due to conservation of angular momentum, rather than being wave-induced. De Verdiere (1979) forced eddies by a zonal series of sources and sinks near the outer edge of the cylinder, and observed retrograde flow in the interior. He also claimed to see a prograde flow at the forcing radii, but does not measure one, nor is one particularly evident in his photographs. McEwan *et al.* (1980) moved the forcing region to mid-radii and, indeed, got a convincing prograde jet over the forcing zone, and show that it is driven by Reynolds stresses. It is shown below, however, that all of the experimental runs reported there were rather strongly nonlinear, so the linear forced-wave theory does not strictly apply. This may be viewed positively, as showing that the theory holds qualitatively into the more realistic nonlinear regime. A much more weakly forced run in the same apparatus is reported here, and the theory is found to hold quantitatively.

The experimental apparatus was a right cylinder of radius $R = 21.4$ cm, rotating with angular velocity Ω and filled with homogeneous water to a depth $H + (\Omega^2/2g)(r^2 - \frac{1}{2}R^2)$ at radius r, with $H = 8$ cm. The bottom is level, and impervious, except in a ring of mean radius $L = 14.25$ cm and width 4.3 cm. This ring is the same level as the rest of the tank, but porous, so water from sources and sinks underneath the foam rubber could leak through. The sources were driven from the sinks, so the total volume remained constant. The numerous tubes for the sources and sinks led through a fluid commutator, so the pattern rotated with respect to the cylinder at angular velocity ω ($\ll\Omega$). No part of the cylinder moved—just the pattern. The water leaking through the foam had no horizontal relative velocity, and there was no net source or sink at any radius integrated over azimuth. Nonetheless, under certain conditions, a strong prograde jet formed over the forcing region.

2. Nondimensional equations

The Navier-Stokes equations for a homogeneous fluid of density ρ and kinematic viscosity ν in a rotating cylindrical coordinate system (r,θ,Z) with relative velocity (V_r,V_θ,V_z) are

$$\frac{\partial V_r}{\partial T} + V_r\frac{\partial V_r}{\partial r} + \frac{V_\theta}{r}\frac{\partial V_r}{\partial \theta} - \frac{V_\theta^2}{r} + V_z\frac{\partial V_r}{\partial Z} = -\frac{1}{\rho}\frac{\partial P}{\partial r} + 2\Omega V_\theta + \nu\left(\nabla^2 V_r - \frac{V_r}{r^2} - \frac{2}{r^2}\frac{\partial V_\theta}{\partial \theta}\right), \quad (2.1)$$

$$\frac{\partial V_\theta}{\partial T} + V_r\frac{\partial V_\theta}{\partial r} + \frac{V_\theta}{r}\frac{\partial V_\theta}{\partial \theta} + V_z\frac{\partial V_\theta}{\partial Z} + \frac{V_\theta V_r}{r} = -\frac{1}{\rho}\frac{1}{r}\frac{\partial P}{\partial \theta} - 2\Omega V_r + \nu\left(\nabla^2 V_\theta + \frac{2}{r^2}\frac{\partial V_r}{\partial \theta} - \frac{V_\theta}{r^2}\right), \quad (2.2)$$

$$\frac{\partial V_z}{\partial T} + V_r\frac{\partial V_z}{\partial r} + \frac{V_\theta}{r}\frac{\partial V_z}{\partial \theta} + V_z\frac{\partial V_z}{\partial Z} = \nu\nabla^2 V_z - \frac{1}{\rho}\frac{\partial P}{\partial Z}, \quad (2.3)$$

$$\frac{\partial(rV_r)}{r\partial r} + \frac{1}{r}\frac{\partial V_\theta}{\partial\theta} + \frac{\partial V_z}{\partial Z} = 0. \quad (2.4)$$

The boundary conditions are

$$V_r = V_\theta = V_z = 0 \quad \text{at} \quad r = R, \quad (2.5)$$

$$V_r = V_\theta = 0 \quad \text{at} \quad Z = 0, \quad (2.6)$$

$$V_z = W_0 F_1(r) F_2(\theta - \omega T) \quad \text{at} \quad Z = 0. \quad (2.7)$$

In addition, there is no stress and

$$P = 0 \quad (2.8)$$

at the free surface

$$Z = H + (\Omega^2/2g)(r^2 - \tfrac{1}{2}R^2) + \eta, \quad (2.9)$$

where

$$V_z = \frac{dZ}{dT} = \frac{d}{dT}[H + (\Omega^2/2g) \times (r^2 - \tfrac{1}{2}R^2) + \eta]. \quad (2.10)$$

We consider n waves around, so the azimuthal length-scale is $l = L/n$. We are interested in quasi-geostrophic flows, so we take the horizontal wave velocity scale as $\delta\Omega l$, with $\delta \ll 1$, and will also require $E = \nu/\Omega H^2 \ll 1$ and $\sigma = n\omega/\Omega \ll 1$. The mean zonal flow scale will be $\Delta\Omega l$, with $\Delta \ll 1$ to be determined.

We define

$$\left.\begin{aligned} \bar{V}_\theta &= \frac{1}{2\pi}\int_0^{2\pi} V_\theta d\theta, \quad V_\theta' = V_\theta - \bar{V}_\theta, \\ \bar{P} &= \frac{1}{2\pi}\int_0^{2\pi} P d\theta, \quad P' = P - \bar{P}, \\ u &= V_\theta'/\delta\Omega l, \quad v = -V_r/\delta\Omega l, \\ \bar{u} &= \bar{V}_\theta/\Delta\Omega l, \quad w = V_z/W_0 \end{aligned}\right\}, \quad (2.11)$$

$$x = n\theta, \quad y = (L - r)/l, \quad z = Z/H, \quad (2.12)$$

$$\left.\begin{aligned} p &= P'/(\delta\rho\Omega^2 l^2), \quad t = n\omega T \\ \bar{p} &= \bar{P}/(\Delta\rho\Omega^2 l^2), \quad \eta' = ng/(\delta\Omega^2 l^2) \end{aligned}\right\}. \quad (2.13)$$

We can transform to the traditional Cartesian beta-plane (y northward) by expanding in the small parameter $l/L = 1/n$, and letting n become large. This is useful not only for comparison with other theories but because the scaling is simplified. The equations become

$$\sigma\frac{\partial u}{\partial t} + \Delta\left(\bar{u}\frac{\partial u}{\partial x} + v\frac{\partial\bar{u}}{\partial y}\right) + \delta\left(u\frac{\partial u}{\partial x} + v\frac{\partial u}{\partial y} + \sigma\delta w\frac{\partial u}{\partial z}\right) - 2v = -\frac{\partial p}{\partial x} + E\frac{\partial^2 u}{\partial z^2} + \left(\frac{H}{l}\right)^2 E\left(\frac{\partial^2 u}{\partial x^2} + \frac{\partial^2 u}{\partial y^2}\right), \quad (2.14)$$

$$\delta\left[\sigma\frac{\partial v}{\partial t} + \Delta\bar{u}\frac{\partial v}{\partial x} + \delta\left(u\frac{\partial v}{\partial x} + v\frac{\partial v}{\partial y} + \sigma w\frac{\partial w}{\partial z}\right) + 2u\right] + 2\Delta\bar{u} = \delta\left[-\frac{\partial p}{\partial y} + E\frac{\partial^2 v}{\partial z^2} + E\left(\frac{H}{l}\right)^2\left(\frac{\partial^2 v}{\partial x^2} + \frac{\partial^2 v}{\partial y^2}\right)\right] - \Delta\frac{\partial\bar{p}}{\partial y}, \quad (2.15)$$

$$\sigma\left(\frac{H}{l}\right)^2\left[\sigma\frac{\partial w}{\partial t} + \Delta\bar{u}\frac{\partial w}{\partial x} + \delta\left(u\frac{\partial w}{\partial x} + v\frac{\partial w}{\partial y} + \sigma w\frac{\partial w}{\partial z}\right)\right] = -\frac{\partial p}{\partial z} + \sigma\left(\frac{H}{l}\right)^2\left[E\frac{\partial^2 w}{\partial z^2} + \left(\frac{H}{l}\right)^2 E\left(\frac{\partial^2 w}{\partial x^2} + \frac{\partial^2 w}{\partial y^2}\right)\right], \quad (2.16)$$

$$\delta\Omega\left(\frac{\partial u}{\partial x} + \frac{\partial v}{\partial y}\right) + \frac{W_0}{H}\frac{\partial w}{\partial z} = 0. \quad (2.17)$$

Taking the curl of (2.14) and (2.15) and substituting in (2.17) shows that the horizontal divergence term is $O(\delta\Omega\sigma)$, hence determining δ from the imposed W_0:

$$\delta = W_0/(\Omega H\sigma) = W_0/n\omega H. \quad (2.18)$$

Thus, the nondimensional form of (2.4) is

$$\frac{\partial u}{\partial x} + \frac{\partial v}{\partial y} + \sigma\frac{\partial w}{\partial z} = 0. \quad (2.19)$$

The boundary conditions become

$$u = v = w = 0 \quad \text{as} \quad y \to \pm\infty, \quad (2.20)$$

$$u = v = 0 \quad \text{at} \quad z = 0, \quad (2.21)$$

$$w = f_1(y) f_2[x - t\ \mathrm{sgn}(\omega)] \quad \text{at} \quad z = 0, \quad (2.22)$$

and there is no stress and

$$p = 0 \quad (2.23)$$

at the free surface

$$z = 1. \quad (2.24)$$

The slope and surface deviation dropped out of (2.24) because we are expanding in $1/n$, and those terms were conveniently $O(1/n)$ and $O(\delta/n^2)$, at least for $\Omega^2 L^2/gH \leqslant 1$, i.e., if the water depth is not zero in the center of the cylinder. The slope is retained in the expansion of (2.10) in $1/n$, i.e.,

$$w = -\tfrac{1}{2}\beta v, \quad (2.25)$$

where (2.18) has been used and

$$\beta = \frac{2\Omega^3 l^2}{|\omega| gH}. \quad (2.26)$$

3. Steady flows

We assume a periodic forcing and steady mean flow, and take a time (or x) average of (2.14)–(2.24):

$$\delta \frac{\partial}{\partial y}(\overline{uv}) + O(\sigma\delta) - 2\bar{v} = O(E) \tag{3.1}$$

$$O(\delta^2) + \Delta 2\bar{u} = -\Delta \frac{\partial \bar{p}}{\partial y} + O(E) \tag{3.2}$$

$$O(\sigma\delta) = -\frac{\partial \bar{p}}{\partial z} + O(\sigma E) \tag{3.3}$$

$$\frac{\partial \bar{v}}{\partial y} + \sigma \frac{\partial \bar{w}}{\partial z} = 0 \tag{3.4}$$

$$\bar{w} = 0 \quad \text{at} \quad z = 0 \tag{3.5}$$

$$\bar{w} = -\tfrac{1}{2}\beta\bar{v} \quad \text{at} \quad z = 1. \tag{3.6}$$

Dropping smaller terms, Eq. (3.1) requires a mean meridional flow for the interior, i.e.,

$$\bar{v} = \tfrac{1}{2}\delta \frac{\partial}{\partial y}(\overline{uv}). \tag{3.7}$$

But in a steady state, this mass flux must come back. The Ekman layer is the only avenue, hence the pressure gradient $\partial\bar{p}/\partial y$ builds up until it forces the return flow to balance. Since the mass flux required is $O(\delta)$ in this scaling, and the Ekman layer is only $O(E^{1/2})$ thick, $\bar{v}$ in the Ekman layer is $O(\delta E^{-1/2})$, and we must rescale:

$$\tilde{v} = -\bar{V}_r/\delta^2\Omega l E^{-1/2}, \quad v = -V_r'/\delta\Omega l, \tag{3.8}$$

$$\xi = Z/E^{1/2}H. \tag{3.9}$$

Substituting in (2.1), dropping $O(1/n)$ as before, and taking a t and x average gives

$$\overline{\delta v \frac{\partial u}{\partial y}} + \sigma\delta E^{-1/2}\overline{w \frac{\partial u}{\partial \xi}} + \delta\Delta E^{-1/2}\left(\bar{v}\frac{\partial \bar{u}}{\partial y} + \tilde{w}\frac{\partial \bar{u}}{\partial \xi}\right)$$
$$-2\delta E^{-1/2}\bar{v} = \frac{\Delta}{\delta}\frac{\partial^2 \bar{u}}{\partial \xi^2} + E\left(\frac{\partial^2 \bar{u}}{\partial y^2} + \frac{\partial^2 \bar{u}}{\partial x^2}\right). \tag{3.10}$$

The Coriolis force term is the largest on the left side of (3.10), and can only be balanced by the frictional term on the right, so

$$\Delta = \delta^2 E^{-1/2}, \tag{3.11}$$

and $\bar{u}$ has the same scale as $\bar{v}$ in the boundary layer, with the difference that $\bar{u}$ extends into the interior. Dropping small terms $O(E^{1/2})$, $O(\sigma)$, $O(\Delta)$ and $O(E^{3/2}\delta^{-1})$ compared to the Coriolis term in (3.10), the analogous equations derived from (2.2) to (2.7) give

$$-2\bar{v} = \frac{\partial^2 \bar{u}}{\partial \xi^2}, \tag{3.12}$$

$$2\bar{u} = -\frac{\partial \bar{p}}{\partial y} + \frac{\partial^2 \bar{v}}{\partial \xi^2}, \tag{3.13}$$

$$0 = -\frac{\partial \bar{p}}{\partial \xi}, \tag{3.14}$$

$$\bar{u} = \bar{v} = 0 \quad \text{at} \quad \xi = 0, \tag{3.15}$$

$$\bar{v} \to 0 \quad \text{as} \quad \xi \to \infty, \tag{3.16}$$

$$\int_0^\infty \bar{v}(y,\xi)d\xi = -\frac{1}{2}\frac{\partial}{\partial y}(\overline{uv}), \tag{3.17}$$

where the last term is the Reynolds stress/mass flux specified by the interior.

The set (3.12)–(3.16) has a simple solution:

$$\bar{u} = \tfrac{1}{2}(e^{-\xi}\cos\xi - 1)\frac{\partial \bar{p}}{\partial y},$$

$$\bar{v} = -\tfrac{1}{2}e^{-\xi}(\sin\xi)\frac{\partial \bar{p}}{\partial y}. \tag{3.18}$$

Substituting in (3.17) determines the pressure gradient

$$\int_0^\infty \bar{v}d\xi = -\frac{1}{4}\frac{\partial \bar{p}}{\partial y} = -\frac{1}{2}\frac{\partial}{\partial y}(\overline{uv}), \tag{3.19}$$

and therefore the interior zonal velocity

$$\bar{u}_\infty = -\frac{1}{2}\frac{\partial \bar{p}}{\partial y} = -\frac{\partial}{\partial y}(\overline{uv}). \tag{3.20}$$

In dimensional (but Cartesian) variables, this is a mean zonal interior flow of

$$\boxed{\bar{u} = -\frac{1}{E^{1/2}\Omega}\frac{\partial}{\partial y}(\overline{uv})} \tag{3.21}$$

This is exactly what one would expect: the mean flow has (is) the amount of momentum accumulated by the Reynolds stress over a spindown time.

The result (3.21) seems to require only quasi-geostrophy, that is, that δ, σ, Δ and E should separately be small. In particular, it can hold for a mean flow stronger than the waves driving it, if $\delta < \Delta \ll 1$. Since $\Delta = \delta^2 E^{-1/2}$, this is the case $E^{1/2} < \delta \ll E^{1/4}$, which is easily attained experimentally, and seems rather realistic for the atmosphere or ocean.

Tractable analytic examples of waves to use in (3.21) will require a further restriction, namely linearity ($\sigma \gg \Delta$ and $\sigma \gg \delta$). Otherwise Doppler shifting and critical layers will complicate matters greatly. However, it is worth emphasizing that this restriction does not apply to the general quasi-geostrophic result (3.21) but only to the example to be worked out in the next section.

Since the experiment was done in a cylinder, it will be useful to also present the result in cylindri-

cal coordinates. The scaling arguments will be used to neglect terms such as the vertical advection, but the equations will be dimensional. Averaging (2.2) over θ and t, the equivalent of (3.7) is

$$\bar{V}_r = -\frac{1}{2\Omega}\left(\overline{V_r \frac{\partial V_\theta}{\partial r}} + \overline{\frac{V_\theta V_r}{r}}\right). \quad (3.22)$$

The Ekman layer must therefore have a radial flux of $-H\bar{V}_r$. The Ekman layer equations have exactly the same form as above, so the pressure gradient is determined by

$$\frac{1}{2}\left(\frac{\nu}{\Omega}\right)^{1/2}\left(-\frac{1}{2\Omega}\frac{\partial \bar{P}}{\partial r}\right) = \frac{H}{2\Omega}\frac{1}{r^2}\frac{\partial}{\partial r}(\overline{r^2 V_\theta V_r}), \quad (3.23)$$

hence the cylindrical analog of (3.21) is

$$\boxed{\bar{V}_\theta = -\frac{H}{(\nu\Omega)^{1/2}}\frac{1}{r^2}\frac{\partial}{\partial r}(\overline{r^2 V_\theta V_r})} \quad (3.24)$$

This expression represents a torque balance, but not quite the convergence of the angular momentum flux because the radially varying depth is outside the derivative.

4. Forced waves

If we subtract the steady parts (3.1)–(3.4) from (2.14)–(2.19), then drop small terms O(δ), O(E) and O(Δ), then we get the quasi-geostrophic wave equations

$$\sigma\frac{\partial u}{\partial t} - 2v = -\frac{\partial p}{\partial x}, \quad (4.1)$$

$$\sigma\frac{\partial v}{\partial t} + 2u = -\frac{\partial p}{\partial y}, \quad (4.2)$$

$$\sigma^2\left(\frac{H}{l}\right)^2\frac{\partial w}{\partial t} = -\frac{\partial p}{\partial z}, \quad (4.3)$$

$$\frac{\partial u}{\partial x} + \frac{\partial v}{\partial y} + \sigma\frac{\partial w}{\partial z} = 0. \quad (4.4)$$

Taking the curl of (4.1) and (4.2) and substituting in (4.4) gives

$$\frac{\partial}{\partial t}\left(\frac{\partial v}{\partial x} - \frac{\partial u}{\partial y}\right) = 2\frac{\partial w}{\partial z}. \quad (4.5)$$

Now we can drop terms O(σ) without losing the time-derivative:

$$v = \frac{1}{2}\frac{\partial p}{\partial x}, \quad u = -\frac{1}{2}\frac{\partial p}{\partial y}, \quad 0 = \frac{\partial p}{\partial z}, \quad (4.6)$$

and w is linear in z. From (2.24) and (2.25),

$$w = -\tfrac{1}{2}\beta v = -\tfrac{1}{4}\beta\frac{\partial p}{\partial x} \quad \text{at} \quad z = 1. \quad (4.7)$$

From (2.22) and the usual Ekman layer,

$$w = f_1(y)f_2[x - t\ \mathrm{sgn}(\omega)] + \frac{1}{4}\frac{E^{1/2}}{\sigma}\left(\frac{\partial^2 p}{\partial x^2} + \frac{\partial^2 p}{\partial y^2}\right)$$

at

$$z = 0. \quad (4.8)$$

The difference between (4.7) and (4.8) is $\partial w/\partial z$; substituting it and (4.6) into (4.5) gives

$$\frac{\partial}{\partial t}\left(\frac{\partial^2 p}{\partial x^2} + \frac{\partial^2 p}{\partial y^2}\right) = -\beta\frac{\partial p}{\partial x} - 4f_1(y)f_2[x - t\ \mathrm{sgn}(\omega)] - \frac{E^{1/2}}{\sigma}\left(\frac{\partial^2 p}{\partial x^2} + \frac{\partial^2 p}{\partial y^2}\right). \quad (4.9)$$

Since (4.9) is linear, we can take a wave form

$$p = \mathrm{Re}\{\hat{p}\exp[i(x - st)]\}, \quad (4.10)$$

with $s = \mathrm{sgn}(\omega)$, so

$$\left(s + i\frac{E^{1/2}}{\sigma}\right)\frac{d^2\hat{p}}{dy^2} - \left(s + i\frac{E^{1/2}}{\sigma} + \beta\right)\hat{p} = -4if_1(y). \quad (4.11)$$

Rhines (1977) has used general arguments to show that outside of the forcing region, the mean flow must be retrograde. That can be seen here, too. Assuming $f_1(y) = 0$ for large $|y|$, boundedness at infinity implies

$$\hat{p} = Ae^{-r|y|}, \quad (4.12)$$

with

$$r = (1 + s\beta)^{1/2}\left(1 - i\frac{1}{2\sigma}\frac{E^{1/2}}{1 + s\beta}\right) + O(E). \quad (4.13)$$

This represents slowly damped oscillations in y for

$$1 + s\beta = 1 + \frac{2\Omega^3 l^2}{\omega g H} < 0,$$

which is

$$-\frac{2\Omega^3 l^2}{gH} < \omega < 0. \quad (4.14)$$

In this case, of slow retrograde forcing, we get waves with backward tilt, i.e.,

$$p = A\sin[(\beta - 1)^{1/2}|y| + x + t] \times \exp[-\tfrac{1}{2}\beta E^{1/2}\sigma^{-1}|y|/(\beta - 1)^{1/2}], \quad (4.15)$$

so

$$v = \tfrac{1}{2}A\cos[(\beta - 1)^{1/2}|y| + x + t] \times \exp[-\tfrac{1}{2}\beta E^{1/2}\sigma^{-1}|y|/(\beta - 1)^{1/2}], \quad (4.16)$$

$$u = -\tfrac{1}{2}A\{(\beta - 1)^{1/2}\cos[(\beta - 1)^{1/2}|y| + x + t] - \tfrac{1}{2}\beta E^{1/2}\sigma^{-1}\sin[(\beta - 1)^{1/2}|y| + x + t]\} \times \exp[-\tfrac{1}{2}\beta E^{1/2}\sigma^{-1}|y|/(\beta - 1)^{1/2}]\,\mathrm{sgn}(y), \quad (4.17)$$

$$\overline{uv} = -\tfrac{1}{8}A^2(\beta - 1)^{1/2} \times \exp[-\beta E^{1/2}\sigma^{-1}|y|/(\beta - 1)^{1/2}]\,\mathrm{sgn}(y). \quad (4.18)$$

Thus the Reynolds stress is toward the forcing region from both sides. Further, it gets stronger as one comes closer, so there is a divergence of the Reynolds stress and from (3.20)

$$\bar{u} = -\tfrac{1}{4}A^2\beta E^{1/2}\sigma^{-1} \times \exp[-\beta E^{1/2}\sigma^{-1}|y|/(\beta - 1)^{-1/2}]. \quad (4.19)$$

This retrograde zonal flow decays rather slowly away from the forcing region, with a rate determined by the friction and the shape of the waves. The amplitude is apparently proportional to $E^{1/2}$ in this scaling, but compared to the perturbation velocities, it is $O(\delta/\sigma)$, so is actually independent of E.

For prograde or rapid retrograde forcing, such that (4.14) does not hold and Rossby waves cannot propagate, Eq. (4.13) represents exponentially trapped motion with a slight backward tilt to lines of constant phase:

$$p = A\cos\left[\frac{\beta E^{1/2}|y|}{2\sigma(1 + s\beta)^{1/2}} + x - st\right]\exp[-(1 + s\beta)^{1/2}|y|]; \quad (4.20)$$

thus

$$\overline{uv} = -\frac{A^2\beta E^{1/2}}{16\sigma(1 + s\beta)^{1/2}} \times \exp[-2(1 + s\beta)^{1/2}|y|]\,\mathrm{sgn}(y). \quad (4.21)$$

Again there is a momentum flux toward the forcing region but it is much weaker and simply due to friction. On the other hand, the flux decays more rapidly as one goes out, so the momentum divergence and induced mean flow

$$u = -\frac{A^2\beta E^{1/2}}{4\sigma}\exp[-2(1 + s\beta)^{1/2}|y|] \quad (4.22)$$

is of the same magnitude as for the propagating wave (with the same A), but is much narrower.

For the rotating cylinder, the analog of (4.7) is

$$V_z = \Omega^2 r V_r/g \quad (4.23)$$

at

$$Z = H = H_0 + \Omega^2(r^2 - \tfrac{1}{2}R^2)/2g.$$

The analog of the vorticity equation (4.9) is

$$\left(\frac{\partial}{\partial T} + \frac{(\nu\Omega)^{1/2}}{H}\right)\left[\frac{1}{r}\frac{\partial}{\partial r}\left(r\frac{\partial P}{\partial r}\right) + \frac{1}{r^2}\frac{\partial^2 P}{\partial\theta^2}\right] = -\frac{2\Omega^3 r}{gH}\frac{1}{r}\frac{\partial P}{\partial\theta} - \frac{4\Omega^2}{H}W. \quad (4.24)$$

Assuming a wave forcing and response

$$(W,P) = \{\hat{w}(r),\hat{p}(r)\}e^{in(\theta - \omega T)} \quad (4.25)$$

results in

$$\left(-in\omega + \frac{(\nu\Omega)^{1/2}}{H}\right)\left[\frac{1}{r}\frac{d}{dr}\left(r\frac{d\hat{p}}{dr}\right) - \frac{n^2}{r^2}\hat{p}\right] = -\frac{2\Omega^3}{gH}in\hat{p} - \frac{4\Omega^2}{H}\hat{w}. \quad (4.26)$$

5. Laboratory experiment

Angus McEwan very kindly ran an experiment to test the above theory. In the bottom of a cylinder of radius 21.4 cm, a number of holes were drilled. Those with radii of 14.25 cm ± 2 cm were connected by nylon hydraulic tubing to a pump and a fluid commutator. Fluid pumped to the commutator produced a cyclic flow through the tubes to create a pattern of sources and sinks with azimuthal wavenumber 6. Rotation of the divider in the commutator caused the pattern to rotate. A porous foam sheet of thickness 1.2 cm lay over the whole bottom, but flow was confined to an annulus of 12.1 cm inner radius and 16.4 cm outer radius, but sealing the remainder of the foam surface with paint. McEwan found that, when the forcing was turned off, the eddies over the unsealed foam spun down with an effective damping constant about three times as large as the Ekman constant.

The cylinder was filled with water to 8 cm above the foam. Velocities were inferred by measuring relative displacements of slightly buoyant polystyrene beads in 0.5 s exposure photographs. The streaks were short enough that the measured velocity (assigned to its mean radius) is Eulerian rather than Lagrangian. Several hundred streaks were digitized from each photograph. The point values of azimuthal velocity u and the product $u'v'$ were smoothed with a parabolic filter of 3 cm radial width. There was a small mean flow with no forcing, apparently due to the axis of rotation not being exactly vertical (Thompson, 1970); this was subtracted out. Figs. 1 and 2 show the results for a run with $\Omega = 4.82\ \mathrm{s}^{-1}$, $H = 7.4$ cm, $W_0 = 0.05$ cm s^{-1} and $n\omega = -0.32\ \mathrm{s}^{-1}$; thus $\beta = 3.3$ and we are in the Rossby wave regime.

There is a good qualitative correspondence between zeros and maxima in $\bar{u}$ and $\overline{u'v'}$. Estimating $\partial(\overline{u'v'})/\partial y$ near 10 cm radius gives $-\partial(\overline{u'v'})/\partial y \div \Omega\bar{u} \approx 0.004$, and near 18 cm gives 0.007, not far from $E^{1/2} = (\nu/\Omega)^{1/2}/H = 0.006$, and thus in reasonable accord with (2.13). McEwan *et al.* (1980) give other examples. Over the foam, $\lambda = -\partial(\overline{u'v'})/\partial y \div \Omega\bar{u} \approx 0.013$, so $\lambda/E^{1/2} \approx 2$, rather smaller than McEwan measured for the eddies.

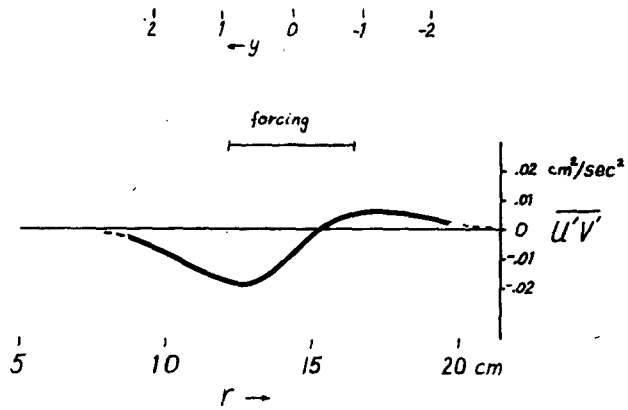

FIG. 1. Measured Reynolds stress $\overline{u'v'} = -\overline{V_\theta V_r}$ vs radius r in a cylinder of radius $R = 21.4$ cm, initial depth $H_0 = 8$ cm, rotation rate $\Omega = 4.82\ s^{-1}$, wavenumber $n = 6$, retrograde forcing at $n\omega = -0.32\ s^{-1}$, and an amplitude $W_0 = 0.05$ cm s^{-1}. Half-second streaks of surface particles gave discrete measurements which were smoothed by a paraboloidal weighting filter of half-width 1.5 cm.

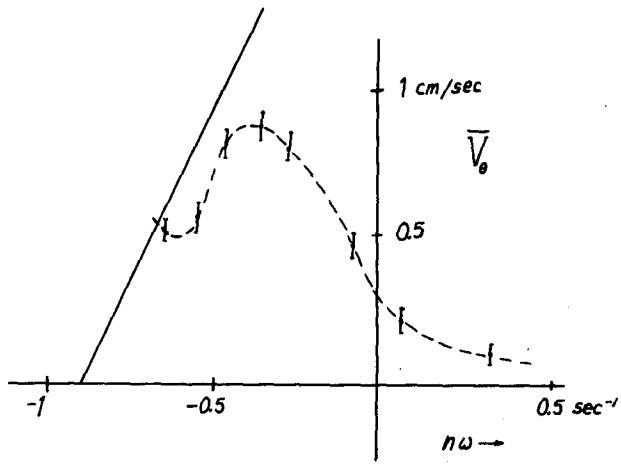

FIG. 3. Measured mean zonal velocity $\bar{V}_\theta$ at $r = 14.25$ cm radius vs $n\omega$ for forcing with amplitude $W_0 = 0.2$ cm s^{-1} in a cylinder of radius $R = 21.4$ cm, initial depth $H_0 = 6$ cm, rotation rate $\Omega = 4.23\ s^{-1}$ and wavenumber $n = 6$.

Fig. 3 shows $\bar{u}$ at $y = 0$ for $\Omega = 4.23\ s^{-1}$, $H = 5.76$ cm, $W_0 = 0.2$ cm s^{-1}, and several values of $n\omega$. Unfortunately, the entire Rossby wave regime ($-0.9\ s^{-1} < \omega < 0$) was not covered, but the trend seems clear. The mean central velocity was prograde for both prograde and retrograde forcing, is less than about 1 cm s^{-1}, and has a finite value as $\sigma = n\omega/\Omega \to 0$.

6. A particular forcing

The foam spreads the effect of each source and sink in an unknown fashion. For an example, it seems reasonable to have continuous $\hat{w}$, rising from zero at the edges to W_0 in the middle. We will consider the problem

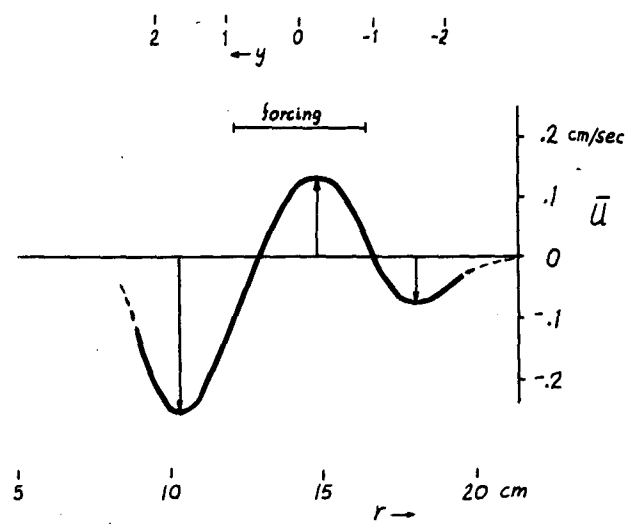

FIG. 2. Measured mean zonal velocity $\bar{V}_\theta$ as for Fig. 1.

$$\left(-s - i\frac{\lambda}{\sigma}\right)\frac{d^2\hat{p}}{dy^2} + \left(s + \beta + i\frac{\lambda}{\sigma}\right)\hat{p} = 4i(1 - y^2/y_0^2) \quad \text{for} \quad |y| < y_0, \tag{6.1}$$

$$\left(-s - i\frac{E^{1/2}}{\sigma}\right)\frac{d^2\hat{p}}{dy^2} + \left(s + \beta + i\frac{E^{1/2}}{\sigma}\right)\hat{p} = 0$$

for

$$|y| > y_0, \tag{6.2}$$

with $\hat{p}$ bounded as $|y| \to \infty$ and $\hat{p}$ and $d\hat{p}/dy$ continuous at $y = \pm y_0$.

The solution can be written

$$\hat{p} = \begin{cases} D_0 + D_2 y^2 \\ \qquad + B(e^{ry} + e^{-ry}), & \text{for} \quad |y| < y \\ Ae^{-\rho(|y| - y_0)}, & \text{for} \quad |y| > y \end{cases} \tag{6.3}$$

where we successively evaluate

$$r = [(s + \beta + i\lambda/\sigma)/(s + i\lambda/\sigma)]^{1/2}, \tag{6.4}$$

$$\rho = [(s + \beta + iE^{1/2}/\sigma)/(s + iE^{1/2}/\sigma)]^{1/2}, \tag{6.5}$$

$$D_2 = -4i/[(s + \beta + i\lambda/\sigma)y_0^2], \tag{6.6}$$

$$D_0 = [4i + 2D_2(s + i\lambda/\sigma)]/(s + \beta + i\lambda/\sigma), \tag{6.7}$$

$$B = (-sD_0 - (sy_0^2 + 2y_0)D_2) \times ((r + \rho)e^{ry_0} + (\rho - r)e^{-ry_0})^{-1}, \tag{6.8}$$

$$A = D_0 + D_2 y_0^2 + B(e^{ry_0} + e^{-ry_0}). \tag{6.9}$$

From (6.3) we can get

$$\overline{u'v'} = \tfrac{1}{8}\,\mathrm{Im}\left(\hat{p}\frac{d\hat{p}^*}{dy}\right)\delta^2\Omega^2 l^2, \tag{6.10}$$

$$\bar{u} = -\tfrac{1}{8}\,\mathrm{Im}\left(\hat{p}\,\frac{d^2\hat{p}^*}{dy}\right) \times \begin{cases} \delta^2\lambda^{-1}\Omega l, & \text{if } |y| < y_0 \\ \delta^2 E^{-1/2}\Omega l, & \text{if } |y| > y_0 \end{cases} \quad (6.11)$$

where the dimensional scales have been appended and the asterisk means complex conjugate.

To compare with Figs. 1 and 2, set $\Omega = 4.82\ \mathrm{s}^{-1}$, $H = 7.4$ cm, $n\omega = -0.32\ \mathrm{s}^{-1}$, $l = 14.25$ cm/6, $y_0 = 2.15$ cm/$l = 0.904$, $W_0 = 0.05$ cm s^{-1}, and $\lambda = 0.012$. The resultant $\bar{u}$ had jumps at $|y| = y_0$, not only due to the change from λ to $E^{1/2}$ in (6.11), but because $d^2\hat{p}/dy^2$ need not be continuous there. The observed $\bar{u}$ was continuous, not only due to Stewartson layers ($E^{1/4}H \approx 0.6$ cm), but because the discrete observed points were smoothed with a filter. The same filter was therefore applied to the results from (6.10) and (6.11), and plotted in Figs. 4 and 5.

The asymmetry between the inner and outer retrograde flows in Figs. 2 and 1 cannot be reproduced by the simple unbounded beta-plane model. Reflection from the relatively nearby outer wall forces $\overline{u'v'} = 0$ at the wall and reduces the net $\overline{u'v'}$ nearby; this may partly explain the asymmetry.

The worst feature of the theoretical prediction is that the rate of decay away from the forcing region is too slow, both for $\overline{u'v'}$ in Fig. 4 and for $\bar{u}$ in Fig. 5. It appears from (4.14) that $\beta \propto r^2$, and so drops to 1 at about $r = 7$ cm. Therefore, the waves cannot penetrate farther in; their group velocity goes to zero, and they are absorbed more quickly than predicted by the beta-plane centered farther out. Their quicker absorption causes the stronger, narrower retrograde jet.

To test this, it was necessary to go back to cylindrical coordinates. To use the same sort of forcing as for (6.1), $\hat{w}$ in (4.26) was taken as

$$\hat{w}(r) = \begin{cases} 0, & \text{if } |r - 14.25| > 2.15 \\ W_0\{1 - [(r - 14.25)/2.15]^2\}, & \text{otherwise.} \end{cases} \quad (6.12)$$

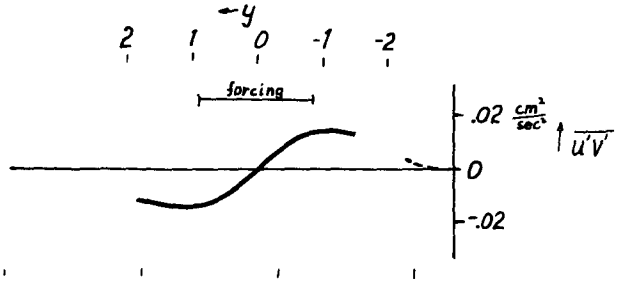

FIG. 4. Computed Reynolds stress $\overline{u'v'}$, from the beta-plane model, with a paraboloidal filter of half-width 1.5 cm, for $n\omega = -0.32\ \mathrm{s}^{-1}$, $\Omega = 4.82\ \mathrm{s}^{-1}$, $h_0 = 7.4$ cm, $\lambda = 0.012$.

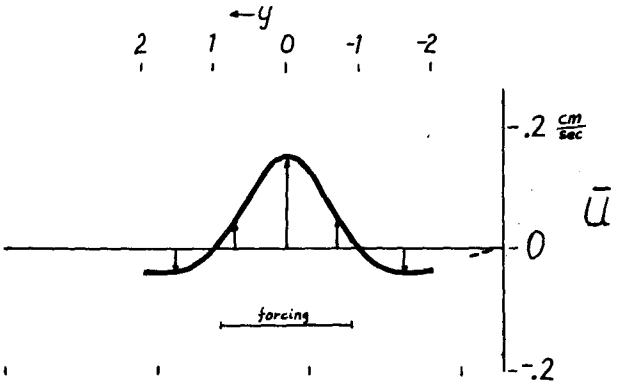

FIG. 5. Computed mean zonal flow $\bar{u}$ as for Fig. 4.

If we now write $B(r) = -in\omega + (\nu\Omega)^{1/2}H^{-1}$, Eq. (4.26) becomes

$$Br\,\frac{d}{dr}\left(r\,\frac{d\hat{p}}{dr}\right) + \left(-n^2B + in\,\frac{2\Omega^3}{gH}\,r^2\right)\hat{p} + \frac{4\Omega^2r^2}{H}\,\hat{w} = 0. \quad (6.13)$$

The boundary conditions $V_r = 0$ at $r = R$, bounded at $r = 0$, become

$$p(R) = 0 \quad p(0) = 0, \quad (6.14)$$

so we have a simple second-order equation with two boundary conditions. Taking $\Delta r = R/N$, $r_j = (j - 1)r$, $H_j = H_0 + \Omega^2(r_j^2 - \tfrac{1}{2}R^2)/2g$, the finite-difference problem is

$$\left.\begin{aligned} &p_1 = 0, \quad p_{N+1} = 0 \\ &C_jp_j + D_jp_{j+1} + E_jp_{j-1} + F_j = 0 \\ &\qquad\qquad \text{for } j = 2(1)N, \end{aligned}\right\}, \quad (6.15)$$

where

$$C_j = -B_j[n^2 + 2(j - 1)^2] + in2\Omega^3r_j^2/gH_j, \quad (6.16)$$

$$D_j = B_jr_j(r_j + r_{j+1})/2(\Delta r)^2, \quad (6.17)$$

$$E_j = B_jr_j(r_{j-1} + r_j)/2(\Delta r)^2, \quad (6.18)$$

$$F_j = 4\Omega^2r_j^2w_j/H_j. \quad (6.19)$$

The tri-diagonal system (6.15) was solved by shooting

$$p_{j+1} = -(C_jp_j + E_jp_{j-1} + F_j)/D_j, \quad (6.20)$$

by assuming $p_2 = 0$ and getting $R_0 = E_Np_{N-1} + C_Np_N$, then assuming $p_1 = 1$ and getting $R_1 = E_Np_{N-1} + C_Np_N$, then setting $p_2 = -R_0/R_1$ and solving. The system (6.15) is diagonally dominant for ω outside the Rossby wave regime [Eq. (4.14)] (and even slightly into it, due to viscosity), and can thus be solved by relaxation. The solutions by the two methods checked exactly to the four decimal

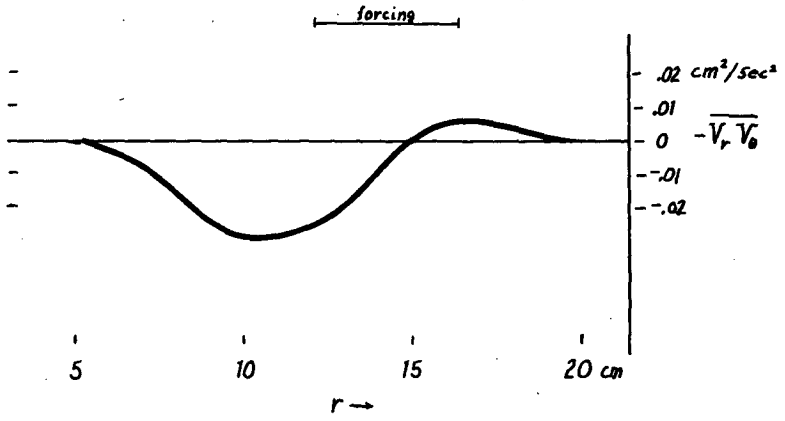

FIG. 6. Computed Reynolds stress $-\overline{V_\theta V_r}$ from the cylindrical model for $n = 6$, $n\omega = -0.32\ s^{-1}$, $\Omega = 4.82\ s^{-1}$, $H_0 = 8$ cm, $\lambda = 3E^{1/2}$.

places printed. Within the regime (4.14), solutions via (6.20) showed no change in behavior in going from $N = 50$ to $N = 70$, so there was apparently no trouble with round-off.

Knowing $\{p_j\}$, one has

$$\overline{V_\theta V_r} = \frac{n}{8\Omega^2 r}\,\mathrm{Im}\left(\hat{p}\,\frac{d\hat{p}^*}{dr}\right), \qquad (6.21)$$

$$\overline{V_r\,\frac{\partial V_\theta}{\partial r}} = \frac{n}{8\Omega^2 r}\,\mathrm{Im}\left(\hat{p}\,\frac{d^2\hat{p}^*}{dr^2}\right), \qquad (6.22)$$

to get $\bar{V}_\theta$ from (3.24). The same case was run as before, $\Omega = 4.82$, $\omega = -0.32/6$, $W_0 = 0.05$, $H_0 = 8$ cm [note: $H(14.25) = 7.4$], but now with the spin-down constant of the foam $\lambda = 3E^{1/2}$. This value is that directly measured by McEwan from the decay rate of eddies after the forcing is turned off, and not adjusted to fit this run, as was done (because it was necessary) for Figs. 4 and 5. Fig. 6 shows the resultant Reynolds stresses, with sign revised to correspond to the rotated coordinates of Fig. 1. Fig. 7 presents $\bar{V}_\theta$ both with and without the data smoothing. The effect of smoothing on Fig. 6 was hardly visible.

The comparison with the experiment is much improved. The prograde and outer retrograde jets are almost exact. The inner retrograde jet is somewhat too strong and too far in, compared to the experiment, but not grossly. Note that the hypothesis seems to be correct that the waves apparently cannot propagate ("tunnel") in much past $r = 6.8$ cm, where the local β drops below 1. This means that the group velocity drops for smaller r, allowing more rapid spatial damping of the waves than predicted by the beta-plane model and, consequently,

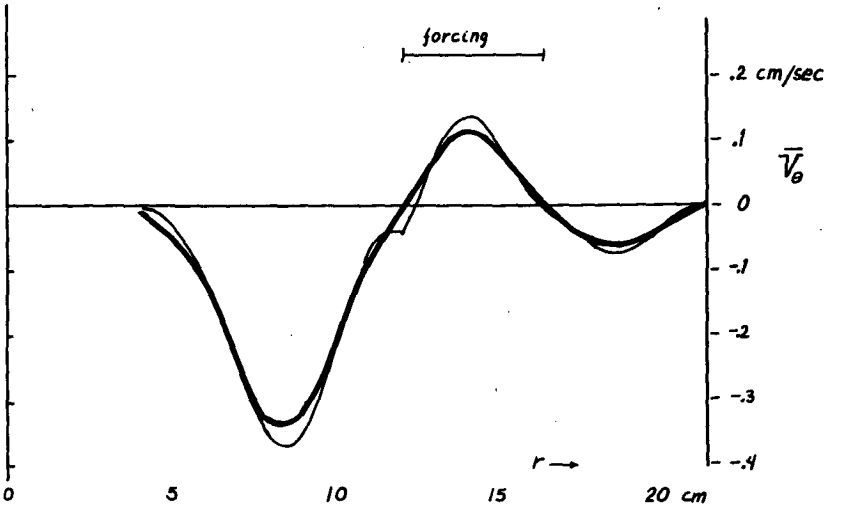

FIG. 7. Computed mean zonal flow $\bar{V}_\theta$ as for Fig. 6. The thin line is unsmoothed, the thick line smoothed with a paraboloidal filter of half-width 1.5 cm.

a more concentrated retrograde jet. Note that no critical layer phenomenon is involved in the theory, and the observed retrograde flow is nowhere as strong as the forcing phase speed ωr, unlike the more strongly forced cases reported by McEwan *et al.* (1981).

Fig. 8 shows the predicted $\bar{V}_\theta$ at $r = 14.25$ versus $n\omega$ for $\Omega = 4.23$, $H_0 = 6$, $W_0 = 0.2$, and $\lambda = 3E^{1/2}$. It does not look much like the observed Fig. 3. McEwan *et al.* (1981) argue that the prograde mean velocity V_θ adds to the retrograde phase speed ωr to form an effective $\beta' = 2\Omega^3 l^2/[gH(r^{-1}V_\theta - \omega)$, and waves cannot propagate for $\beta' < 1$, or

$$n\omega < -0.907 + \bar{V}_\theta/2.38 \qquad (6.23)$$

in this case. Therefore, one expects the observed $\bar{V}_\theta$ not to rise above the line (6.23) marked on Fig. 8, which cuts off the left peak. This argument probably has some truth. However, one need not go to this level of sophistication, for the quasi-linear wave theory does not apply near either peak; the forcing $W_0 = 0.2$ cm s^{-1} is too strong, and the particle speeds (from the linear theory) exceed 50% of the phase speed $|\omega r|$ everywhere except the far left, the far right, and the very bottom of the valley (near $n\omega = -0.5$). In fact, for the entire right peak, the linear V_θ' gets quite large and ω gets small, and $|V_\theta'/\omega r|$ exceeds 1, so there are parcels of fluid trapped in closed streamlines moving with the phase speed. One expects eddies to be much less efficient than waves in transporting momentum, and one thus expects smaller $\bar{V}_\theta$ than predicted by the wave theory.

De Verdiere's (1979) wave steepness $|V'/\omega r|$ is quoted as 3.3, so the forcing is more like closed circular eddies than the waves discussed in this section. In fact, he quotes a volume flux of 363 cm^3 s^{-1} from 36 sources, or 10.1 cm^3 s^{-1} apiece, spaced 2.35 cm apart under foam 2 cm thick. One expects $W_0 \approx (10 \text{ cm}^3 \text{ s}^{-1})/(2 \text{ cm} \times 2 \text{ cm}) \approx 2.5$ cm s^{-1}, and a Rossby number $\delta \approx (2.5)/(0.4 \times 11) \approx 0.5$, which suggests that the flow is not even particularly geostrophic.

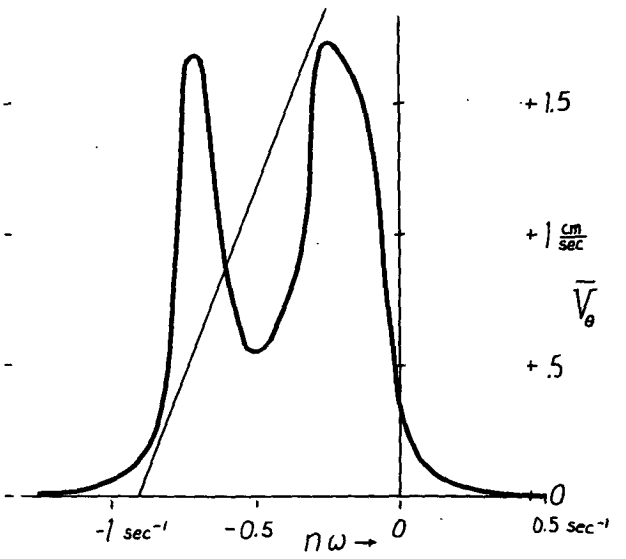

FIG. 8. Computed mean zonal velocity $\bar{V}_\theta$ at $r = 14.25$ cm vs $n\omega$ for $W_0 = 0.2$ cm s^{-1}, $R = 21.4$ cm, $H_0 = 6$ cm, $\Omega = 4.23$ s^{-1}, $n = 6$.

7. Conclusion

The cylindrical coordinates and finite outer radius were necessary to get quantitative agreement of theory with observation. This suggests that a beta-plane will not give very good results on a finite sphere either. The details of the waves also depend on linearity, which is usually not a good approximation for real geophysical fluids. However, it is encouraging that the theory correctly predicts at least the direction of flow for the rather nonlinear experiments of Whitehead (1975), McEwan *et al.* (1980) and De Verdiere (1979), so we can believe that there is some application of the quasi-linear theory presented here to the real world. This supports Thompson's (1971) suggestion that "negative viscosity" is due to the general property of Rossby waves (for positive β) that the meridional component of the momentum flux has a sign opposite to that of the meridional component of the energy flux.

Another basic result here is that the mean zonal flow is the convergence of the Reynolds stress over a spindown time [(3.21) or (3.24)] and this should be quite robust, requiring only quasi-geostrophy. For instance, it allows a mean flow strong compared to the eddies driving it.

We now try applying reasonable cyclone scales for the eddies and see if this theory could explain the jet stream. An energy-releasing scale is $l \approx 1000$ km, which is a wavelength of around 6000 km, or wavenumber 6 in midlatitudes. For this scale, a reasonable vertical velocity W_0 may be 1 cm s^{-1}, and cyclone period may be 6 days, so $n\omega \approx 2\pi/6$ days $\approx 10^{-5}$ s^{-1}. This gives $\delta = W_0/(n\omega H) \approx 0.1$, so the motion is quasi-geostrophic. A spindown time for these large-scale cyclone waves may be $(E^{1/2}\Omega)^{-1} \approx 5$ days (Williams, 1978). From (3.11), $\Delta = \delta^2 E^{-1/2} \approx (0.01)(25) = 0.25$, so the mean zonal velocity scale is $(0.25)(\frac{1}{2} \times 10^{-4} \text{ s}^{-1})(1 \times 10^6 \text{ m}) \approx 12$ m s^{-1}, which is about right for the mean vertically averaged zonal flow in the atmosphere. There may be something to this.

Acknowledgments. Angus McEwan very kindly made and conducted the experiment at CSIRO Division of Atmospheric Physics. This work was started while visiting Monash University, and I thank Bruce Morton and Andy Bennett for their

hospitality. The production of the paper was aided by ONR Contract N00014-75-C-0201.

REFERENCES

De Verdiere, Alain Colin, 1979: Mean flow generation by topographic Rossby waves. *J. Fluid Mech.*, **94,** 39–64.

Eliassen, A., and E. Palm, 1960: On the transfer of energy in stationary mountain waves. *Geofys. Publ.*, **22,** 1–23.

Green, J. S. A., 1970: Transfer properties of large-scale eddies and the general circulation of the atmosphere. *Quart. J. Roy. Meteor. Soc.*, **96,** 157–185.

Held, Isaac M., 1975: Momentum transport by quasi-geostrophic eddies. *J. Atmos. Sci.*, **32,** 1494–1497.

Holopainen, E. O., 1978: On the dynamic forcing of the long-term mean flow by the large-scale Reynolds stresses in the atmosphere. *J. Atmos. Sci.*, **35,** 1596–1604.

Kuo, H.-L., 1951a: Vorticity transfer as related to the development of the general circulation. *J. Meteor.*, **8,** 307–315.

——, 1951b: A note on the kinetic energy balance of the zonal wind systems. *Tellus*, **3,** 205–207.

——, 1953: On the production of mean zonal currents in the atmosphere by large disturbances. *Tellus*, **5,** 344–362.

Mak, Man-Kin, 1969: Laterally driven stochastic motions in the tropics. *J. Atmos. Sci.*, **26,** 41–64.

McEwan, Angus D., Rory O. R. Y. Thompson and R. Alan Plumb, 1981: Mean flows driven by weak eddies in rotating systems. Submitted to *J. Fluid Mech.*

Rhines, Peter B., 1977: The dynamics of unsteady currents. *The Sea*, Vol. 6. Interscience, 189–318 (see pp. 283–294).

——, 1979: Geostrophic turbulence. *Annual Review of Fluid Mechanics.*, Vol. 11, Annual Reviews, 401–441.

Starr, Victor P., 1968: *Physics of Negative Viscosity Phenomena.* McGraw-Hill, 256 pp.

——, and Robert M. White, 1951: A hemispheric study of the atmospheric angular momentum balance. *Quart. J. Roy. Meteor. Soc.*, **77,** 215–225.

Taylor, G. I., 1915: Eddy-motion in the atmosphere. *Phil. Trans. Roy. Soc. London*, **A240,** 1–26.

Thompson, Rory, 1970: Diurnal tides and shear instabilities in a rotating cylinder. *J. Fluid Mech.*, **40,** 737–751.

——, 1971: Why there is an intense eastward current in the North Atlantic but not in the South Atlantic. *J. Phys. Oceanogr.*, **1,** 235–237.

——, 1978: Reynolds stress and deep counter-currents near the Gulf Stream. *J. Mar. Res.*, **36,** 611–615.

Whitehead, Jack A., 1975: Mean flow generated by circulation on a β-plane: An analogy with the moving flame experiment. *Tellus*, **27,** 358–364.

Williams, Gareth P., 1978: Planetary circulations: 1. Barotropic representation of Jovian and terrestrial turbulence. *J. Atmos. Sci.*, **35,** 1399–1426.